F. M. Lay
C. K. Chu
P. H. Haberland

Simulation of Cyclic Operation of a Gas Panel Device

Abstract: This paper presents a numerical simulation model for the operation of a gas panel discharge cell with a neon-argon mixture. The model is based on a Townsend avalanche or direct ionization mechanism and secondary emission, as well as Penning collisions or indirect ionization. Charges on the dielectric walls are included, but space-charge field distortion is neglected. Cyclic operation of the cell is studied in detail and the effects of geometric and electrical parameters (e.g., gap and pulse widths) on the operating characteristics of the cell (e.g., write, sustain and erase voltages) have been obtained. The results are in good agreement with experimental data where available.

Introduction

The gas discharge panel described by Bitzer and Slottow [1] is a display device, consisting essentially of an array of discharge cells which are selectively lit from external electrical circuitry. A more recent design [2] is shown in Fig. 1. Each discharge cell is formed in the gap at the intersection of a set of x-conductor lines (shown as the lower metal electrode at the bottom of the lower figure) and a perpendicular set of y-conductor lines (upper metal electrode on the lower figure). Appropriate voltages are applied to each of the conductors, so that a desired voltage appears across the gap at each intersection or cell, which may initiate a discharge "write", maintain a discharge "sustain", or terminate a discharge "erase". The conductors are embedded in a thin dielectric layer, on which electric charges accumulate and play an essential role in the operation of such a discharge cell. Figure 2 shows such a single cell schematically. The bistable nature of such cells has been described by Bitzer and Slottow [1], Criscimagna [3], and others.

In this paper, we present a one-dimensional time-dependent numerical simulation of the cyclic operation of a gas panel discharge cell. The purpose of this study is to obtain a better physical understanding of the cell operation, thereby permitting easier design improvements. In particular, the model enables us to ascertain the influence of the various cell parameters (e.g., width of gap, dielectric properties, emission coefficient of the glass) and the electrical parameters (e.g., width of the voltage pulses) on the operating characteristics of the cell (e.g., the write voltages V_w sustain voltages V_s erase voltages V_e, the operational margin or difference between the maximum and minimum V_s). The model has permitted us thus far to provide qualitatively correct prediction and interpretation of the cell operation and also some quantitative agreement with experimental results.

Our model assumes one-dimensional variation in all the quantities, such as number density, the variation being in the direction of the gap, perpendicular to the electrodes. Thus we ignore the interaction between adjacent cells. The numerical procedure is identical to that used in our previous paper [4], except that wall charges are now included. The voltage across the gap is a function of both the external voltage and the wall charges, whereas previously there was no dielectric and the voltage across the gap was just the external voltage. We also consider a Ne-Ar (Penning) mixture and take into account both the decay of the metastable neon atoms via three-body and Penning collisions and the generation of new metastable neon atoms. The metastable atoms are a source of electrons during decay and hence play a dominant role in the operation of the cell. The present paper is the only study to our knowledge of multiple-cycle operations.

Our model neglects the space-charge field. This is in contrast to the work of Vernon and Wang [5] and Lanza [6], in which the effect of space charge is included but the role of the metastable atoms is neglected. The space charge distortion indeed has a strong effect on the current pulse, but has a weak influence on V_w, V_s, V_e, and operational margin. On the other hand, the impor-

tance of the metastable atoms is recognized by all workers in the subject. Hence, to produce a manageable model, we have included that effect rather than space charge for the present time. The quantities that particularly interest us are probably well approximated without space charge being included.

In the next section, the equations and numerical procedure are presented and further detailed discussion is given on the assumptions. The subsequent section describes the results: We first give the details of the time-dependent cyclic operations and then summarize the effects of the various parameters on the operating characteristics. Whenever available, comparison is made with experimental results.

Equations and numerical procedure

When space charge is ignored, the equations governing the one-dimensional non-steady-state motion of the ions (subscript i), electrons (subscript e), and metastable atoms (subscript m) are extremely simple. The ion velocity $v_i(t)$ and electron velocity $v_e(t)$ are both uniform in space and depend only on the mobilities μ and the instantaneous uniform electric field $E(t)$. For our calculations, the ion mobility μ_i is taken to be 7 $cm^2 \cdot (s \cdot V)^{-1}$ at 8×10^4 Pa (600 Torr) [7]. Thus

$$v_i = -\mu_i E = -(4200/P)E, \tag{1}$$

$$v_e = +\mu_e E, \text{ and} \tag{2}$$

$$E = V/d, \tag{3}$$

where V is the potential difference across the cell, d is the width of the cell gap and P is the pressure of the gas in the panel.

The ion, electron, and metastable atom densities are all functions of both space and time: $n_i = n_i(x, t)$, $n_e = n_e(x, t)$, $n_m = n_m(x, t)$. They satisfy the particle conservation or continuity equations:

$$\partial n_i/\partial t + v_i \partial n_i/\partial x = \nu_{ee} n_e + \nu_{me} n_m, \tag{4}$$

$$\partial n_e/\partial t + v_e \partial n_e/\partial x = \nu_{ee} n_e + \nu_{me} n_m, \text{ and} \tag{5}$$

$$\partial n_m/\partial t = \nu_{em} n_e - \nu_{me} n_m - \nu_{m3} n_m. \tag{6}$$

The coefficients ν_{ee}, ν_{em}, ν_{me}, and ν_{m3} are the rates of generation, respectively, of ion pairs by electron ionization, of metastable atoms by electron excitation, of ion pairs by metastable decay, and of metastable atom destruction.

The electrodes of the gas cell are coated with a dielectric layer. Thus the voltage V across the cell has to be determined together with the particle densities and velocities and the surface charges Q_a (anode) and Q_c (cathode):

$$\partial Q_a/\partial t = e n_e(d, t) v_e(t), \tag{7}$$

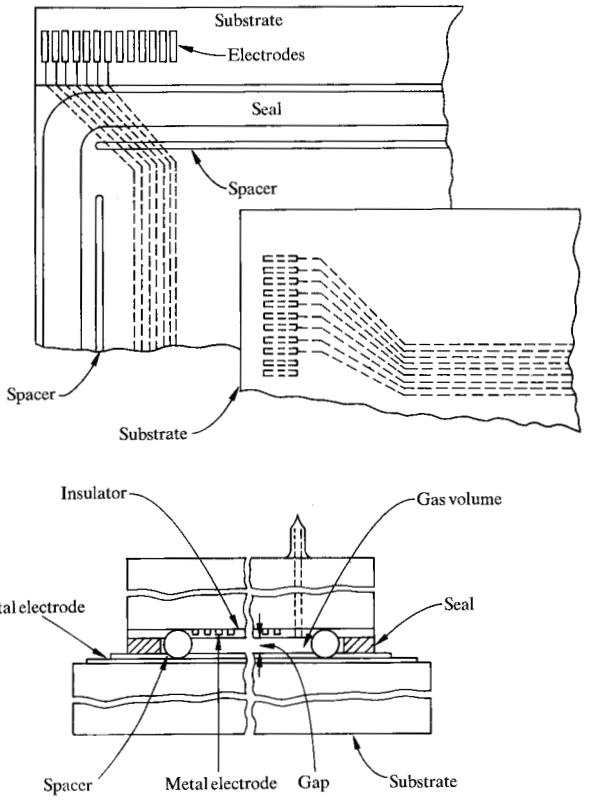

Figure 1 Magnified view (above) and across section (below) of the ac-operated gas panel device.

Figure 2 Simplified diagram of the discharge cell.

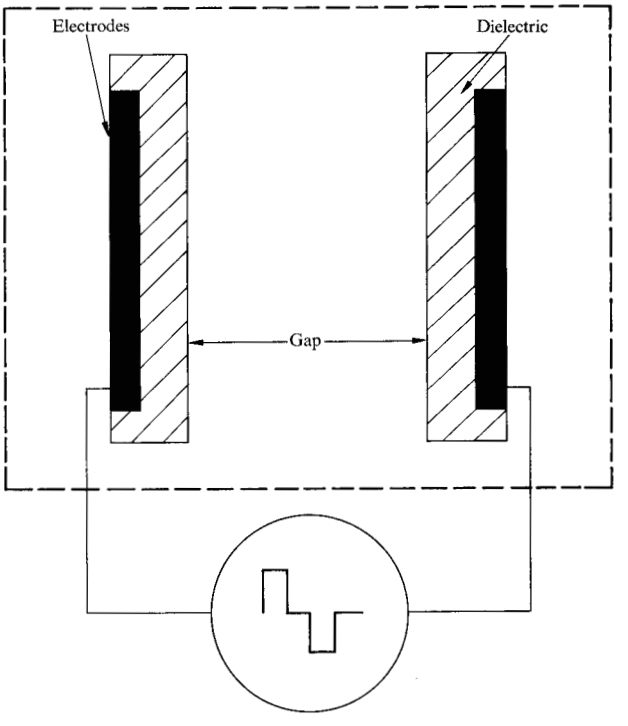

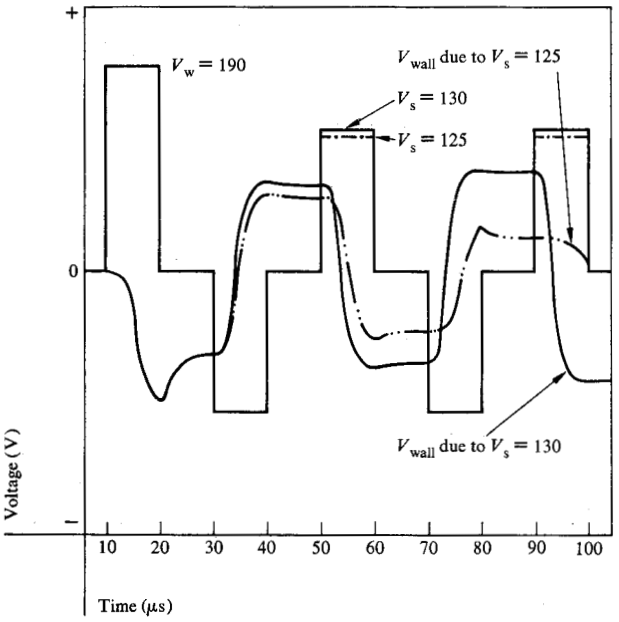

Figure 3 Minimum sustain voltage for write voltage of 190 V.

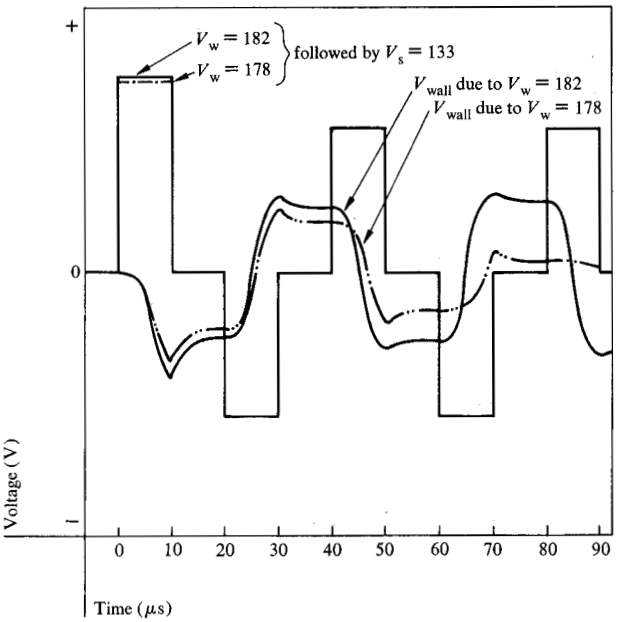

Figure 4 Minimum write voltage for sustain voltage of 133 V.

$$\partial Q_c/\partial t = en_i(0, t)v_i(t), \text{ and} \tag{8}$$

$$V = V_a - (Q_c - Q_a)/C_d. \tag{9}$$

Here V_a is the externally applied voltage and C_d is the capacitance of the dielectric layer. The cathode is at $x = 0$ and the anode is at $x = d$.

The set of equations (1)-(9) is subject to the initial conditions

$$\begin{cases} n_e(x, 0) = n_m(x, 0) = Q_a(0) = Q_c(0) = 0 \text{ and} \\ n_i(x, 0) \approx 10 \text{ ions/cm}^3 \end{cases} \tag{10}$$

and the boundary conditions

$$\begin{cases} n_i(d, t) = 0 \text{ at the anode and} \\ v_e n_e(0, t) = \gamma_i n_i(0, t) v_i(t) \text{ at the cathode,} \end{cases} \tag{11}$$

where γ_i is the secondary emission coefficient.

These equations for a gas cell differ from those for a discharge between two plane electrodes [5] in only one respect. In the latter case the potential difference across the gap is always V_a, whereas in the present case, the potential difference across the gap is V, which is determined by Eqs. (7)-(9). The dielectric layer on the electrodes permits accumulation of charge and shielding of part of the applied voltage.

The secondary emission coefficient due to ion bombardment of the cathode is treated as an adjustable parameter, so that a reasonable breakdown voltage can be obtained from the calculation and compared with experimental values. In the subsequent calculations, γ_i is taken to be $0.01(E/P)^{0.533}$. This exponential form approximates the result shown in Fig. 7 of Ref. [8].

The dielectric capacitance C_d is calculated from an effective area $A + 2wd$, where w is the width of the electrode. The term $2wd$ is added to account for the spreading of the glow discharge.

Based on a three-body collision coefficient of 5×10^{-34} cm$^6 \cdot$ s^{-1} [9] and a Penning collision cross section of 3.46×10^{-16} cm^2 [10] in Ne-Ar, ν_{me} and ν_{m3} are taken to be 10^6 s^{-1} and 5×10^5 s^{-1} at 8×10^4 Pa (600 Torr), respectively. For the metastable atom excitation rate ν_{em}, it is assumed that the number of atoms being excited to metastable states is proportional to the number of atoms being ionized. Klein [11] has derived an expression for this proportionality as a function of the experimentally determined ionization coefficients η_{Ne} of pure neon and $\eta_{Ne\text{-}Ar}$ of a neon-argon mixture. Combining this expression with Eqs. (4) and (5) for steady state operation, one obtains the proportionality constant

$$K = \frac{\nu_{me} + \nu_{m3}}{\nu_{me}} \left(\frac{\eta_{Ne\text{-}Ar}}{\eta_{Ne}} - 1 \right). \tag{12}$$

To obtain a numerical solution for these equations (1) to (9) by a finite-difference method, an approximation must be made because of the great difference in magnitude between electron and ion mobilities. For accurate electron dynamics, the time steps must be a fraction of an electron transit time; but this would necessitate an unreasonably large number of time steps to see any

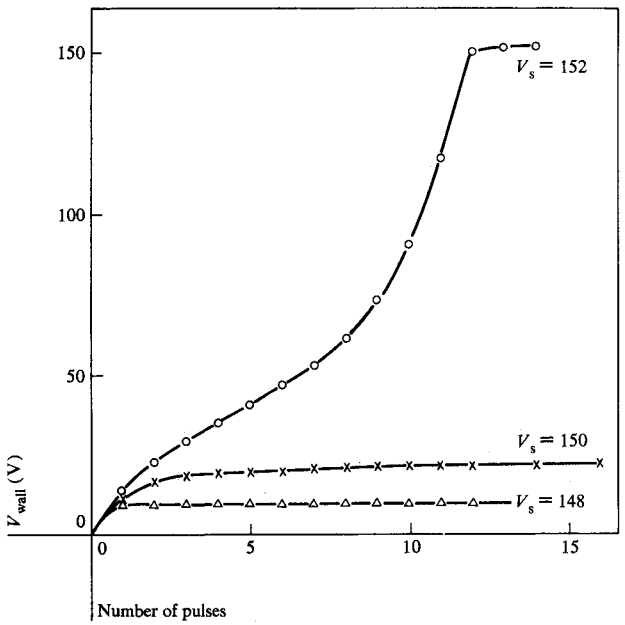

Figure 5 Effect of sustain voltage and number of sustain pulses on the accumulation of wall voltage.

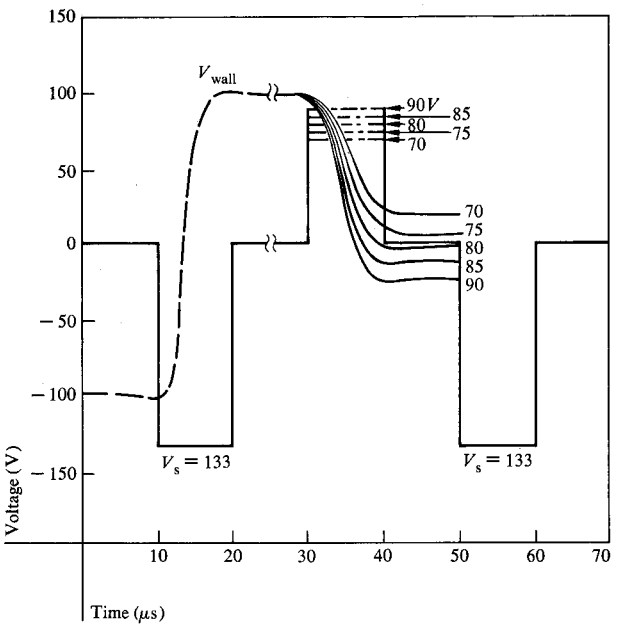

Figure 6 Effect of different V_e on erasure.

phenomenon on the ion time scale. It is better, therefore, to take the time step Δt to be a fraction of the ion transit time and to assume that all the electrons generated during this time are completely collected at the anode, i.e., that they have infinite speed. This approximation sacrifices detailed electron dynamics but maintains the correct cumulative electron behavior at the end of each time step, which typically is 2×10^{-8} s.

The numerical method chosen is a particle-in-cell procedure identical to that described previously by Lay and Chu [5], except that in the present study the wall charges Q_a and Q_c and the voltage V are also calculated at each time step.

Results and discussion

Figures 3 through 7 show the results of the simulation for time dependent cyclic operation of the gas panel device. In Fig. 3 a write pulse of 190 V. is followed by two series of sustain pulses of 130 and 125 V. The pulses are shown as square waves which have a finite rise rate of 0.5×10^9 V · s^{-1}. The responses (two series of smooth-curve pulses) are represented by the counter voltage at the wall, $V_{wall} = -(V_a - V)$ in Eq (9). With a 190-V write pulse, the wall counter voltage builds up, and by the time V_w steps down to zero, the metastable atom density is maximum and the charged particles are subjected to a reverse field. If a sustain pulse train of 130 V is then applied, a dynamic equilibrium is achieved after several pulses. Thus a cell is changed from the off state to the on state. If a sustain voltage of 125 V is used instead, V_{wall} diminishes and the cell remains in the off state. A minimum sustain voltage thus exists for a given V_w, below which a cell cannot be changed from the off state to the on state.

Conversely, for a given V_s, there is a minimum V_w, below which a cell cannot change from the off state to the on state. Figure 4 shows that for V_s of 133 V, the V_{w-min} is about 180 V.

For a given cell, there is also a maximum V_s that can be used, above which all cells change to the on state even if no V_w is applied. Figure 5 is a plot of the cumulative magnitude of the wall voltage after a number of sustain pulses (but no write pulse) have been applied. From the plot it is clear that the breakdown voltage V_{s-max} is about (151 ± 1)V for the particular wave form and frequency used. Above this voltage the cell is in the on state from V_s alone.

To erase a cell, a smaller voltage pulse V_e is applied in place of a regular V_s pulse. Stable operation of the on state is perturbed and this leads to an erasure of the on cell. Figure 6 indicates that a 79-V pulse gives complete erasure in this case. A smaller voltage leaves some residual wall charge, whereas a larger voltage gives a wall charge of the opposite sign.

In addition to minimum V_s and V_w and maximum V_s, there is a maximum V_w. If a write voltage is too high, e.g., $V_w = 230$ V in Fig 7, the metastable atom density increase so much that the step-down of V_w causes a se-

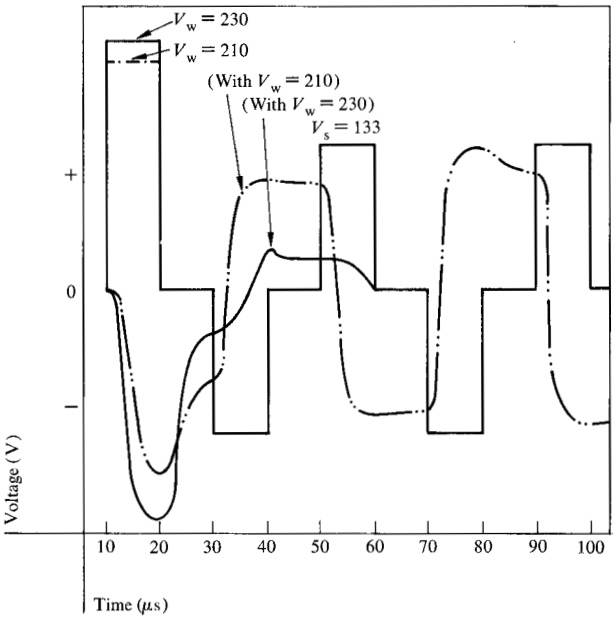

Figure 7 Maximum write voltage for sustain voltage of 133 V.

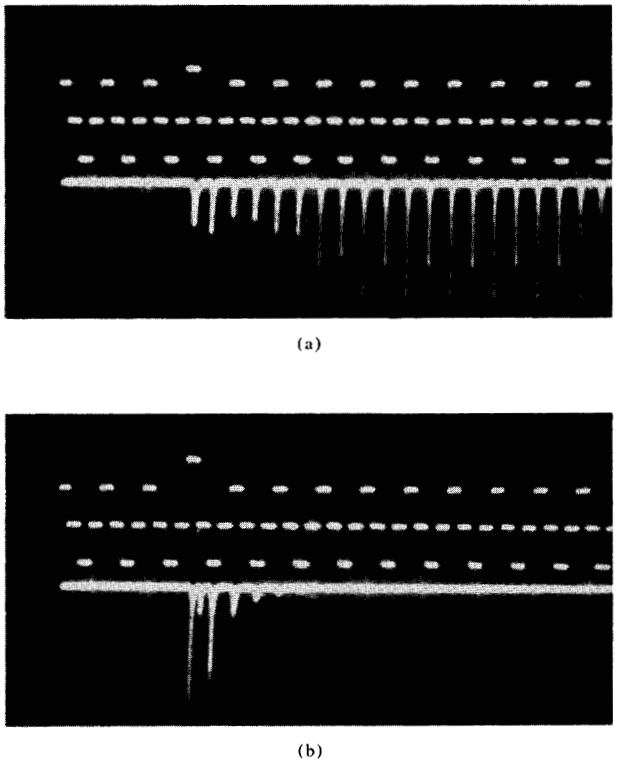

(a)

(b)

Figure 8 Experimental traces of maximum write voltage for a cell sustained at 140 V. The seventh pulse indicates the write voltage: plate (a) $V_w = 194$ V; (b) $V_w = 250$ V. These V_w did not change the cell from the off state.

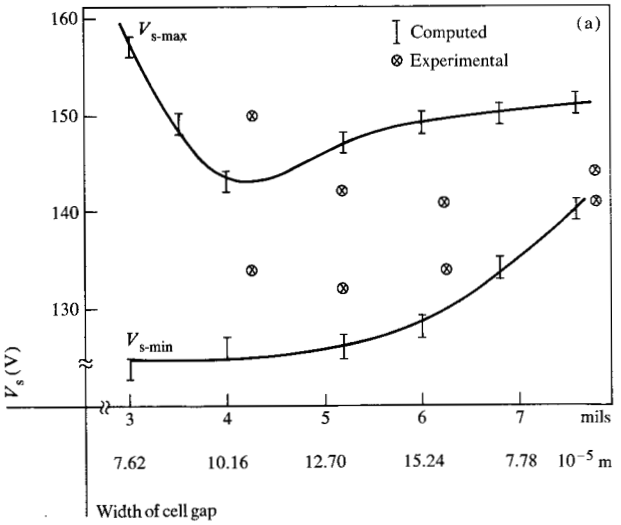

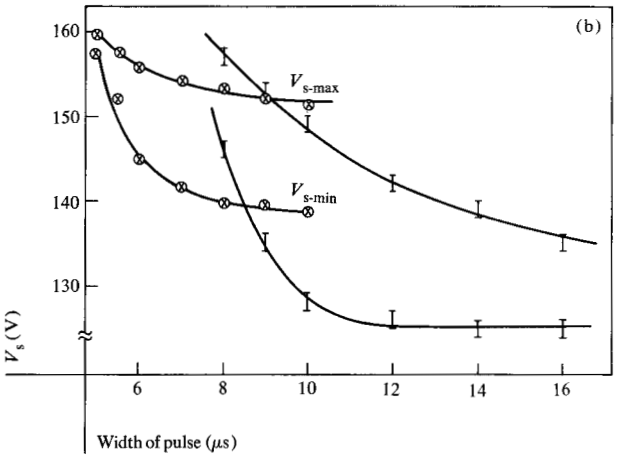

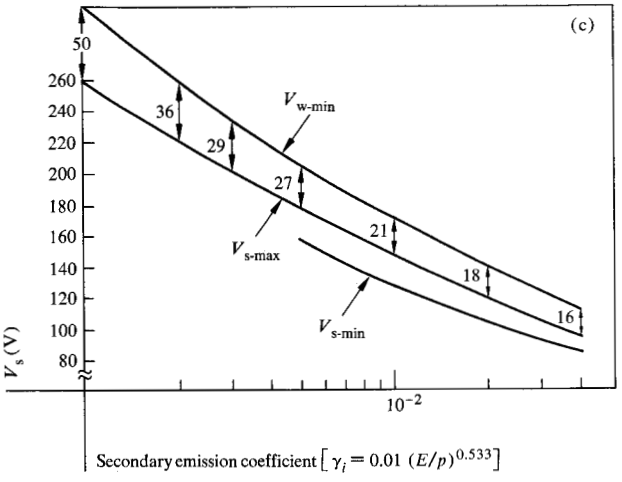

Figure 9 Effects of physical parameters on the sustain voltage: (a) gap width; (b) pulse width; and (c) secondary emission coefficient. The curves with error bars are calculated values and the circles are experimental values.

vere reduction of the wall charge before V_s is applied. The net wall voltage added to the second pulse is, in fact, smaller than that from a lower write voltage. Therefore, for a given V_s if the write voltage exceeds a threshold V_{w-max}, the cell again does not change from an off state to an on state.

Qualitative agreement for the existence of V_{w-max} from experimental results is shown in Fig. 8. To obtain the experimental results an ac square wave pulse train was applied to a cell free from any wall charges and metastable atoms, but containing some initiatory charged particles; the pulse width was 10 Ms and the frequency 25 kHz. The light output was monitored by a photomultiplier tube focused on one cell. The output amplitude is shown in the lower traces of plates (a) and (b). The upper traces of both plates represent the sustain voltage of 140 V, applied to a panel at different times, except for the seventh pulse which is indicated as $V_w = 194$ V for plate (a) and $V_w = 250$ V for plate (b). For a V_s of 140 V, a V_w of 194 V, leads to a dynamically stable on state, but a $V_w = 250$ V does not change the cell from the off state.

Shown in Fig. 9 are the effects of chamber gap, pulse width, and secondary emission coefficient on V_s. The difference $V_{s-max} - V_{s-min}$ is the operational margin. In Fig. 9(a) the experimental curves show that the operational margin becomes very small for large gaps. This might be due to interaction with the adjacent cells ("cross-talk" problem). Figure 9(b) shows general qualitative agreement between simulation and experiment in the effect of pulse width on operational margin. Figure 9(c) shows the effect of γ_i; here no experimental value is available. Note that γ_i has a greater effect on V_w than on V_s. Specifically, as γ_i decreases V_w increases more rapidly than does V_s.

Figure 10 shows the effect of V_s on V_w. For given values of V_s on the abscissa, V_w must lie in that range of the ordinate between the corresponding V_{w-max} and V_{w-min}, i.e., inside the curved region. The difference $V_{w-max} - V_{w-min}$ is, in fact, the operational margin for the write pulse. Again, there is qualitative agreement with experiments.

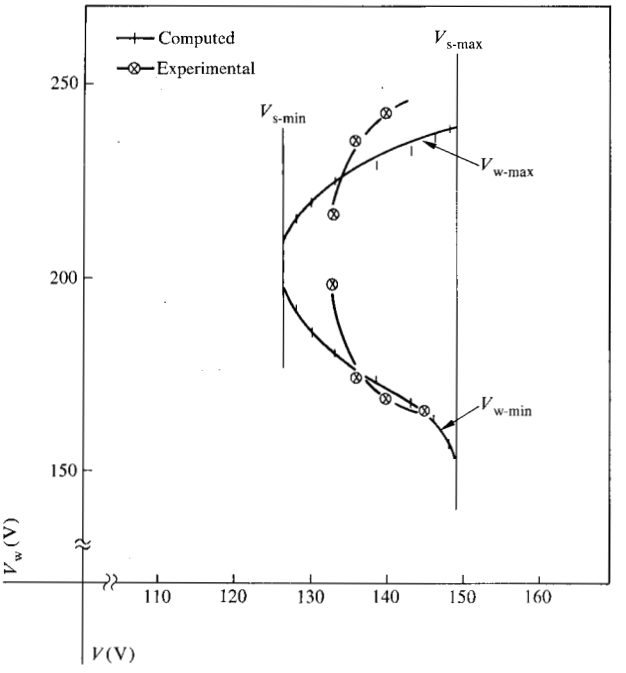

Figure 10 Operational margins for write and sustain voltages.

Acknowledgments

The authors sincerely acknowledge the valuable discussions and helpful assistance of M. Klein, C. Lanza, A. Piston, T. Criscimagna and A. Fiacco during the course of this work.

References

1. D. L. Bitzer and H. G. Slottow, "The Plasma Display Panel," *AFIPS Conference Proceedings, Fall Joint Computer Conference* **29,** 54 (1966).
2. J. F. Nolan, "Gas Discharge Display Panel, "IEEE International Electron Devices Meeting, Washington, D.C., October 1969, p. 54; H. J. Hoehn and R. A. Martel, "A 60 Line Per Inch Plasma Display Panel," *IEEE Trans. Electron Devices* **ED-18,** 659 (1971).
3. T. N. Criscimagna, "Additive Pulses Turn on Display Cells Reliably," *Electro-Optical System Design* **3,** 32 (August 1971).
4. F. M. Lay, and C. K. Chu, "Simulation of a Transient DC Breakdown in a Penning Mixture Between Two Closely Spaced Parallel Electrodes," *J. Appl. Phys.* **44,** 4008 (1973).
5. H. Veron, and C. C. Wang, "AC Electrical Breakdown of Neon With External Electrodes," *J. Appl. Phys.* **43,** 2664 (1972).
6. C. Lanza, "A One-Dimensional Numerical Analysis for an AC Gas Display Panel," *IBM J. Res. Develop.* **18,** 232 (1974); this issue.
7. H. J. Oskain "Microwave Investigation of Disintegrating Gaseous Discharge Plasmas," *Philips Res. Rep.* **13,** 335 (1958).
8. A. A. Kruithof and F. M. Penning, *Physica (Utr.)* **4,** 340 (1937).
9. A. V. Phelps, "Diffusion, De-excitation, the Three Body Collision Coefficients for Excited Neon Atoms," *Phys. Rev.* **114,** 1011 (1959).
10. T. Sinda, "Etude de la Production d'ions par Effect Penning," *Physics Letters* **33A,** 225 (1970).
11. M. Klein, private communication.

Received November 15, 1973

F. M. Lay and P. H. Haberland are located at the IBM System Development Division laboratory, Kingston, New York 12401; C. K. Chu is a professor of engineering science at Columbia University, New York, and a consultant to IBM.